Int. J. Electrochem. Sci., 14 **(2019)** 886 – 896, doi: 10.20964/2019.01.99

International Journal of
ELECTROCHEMICAL
SCIENCE
www.electrochemsci.org

Short Communication

Effects of Three Kinds of Hydrocarbon Degrading Bacteria on Biocorrosion Behavior of 16Mn Steel in the Bacteria-Containing Media

Xiaodong Zhao[1,*], *Kefeng Chen*[2,3], *Jie Yang* [1 *], *Guangfeng Xi*[4], *Haitao Tian*[1], *Qingguo Chen*[2]

[1] School of Ocean, Yantai University, Yantai 264005, China;
[2] School of Naval Architecture and Mechanical-electrical Engineering, Zhejiang Ocean University, Zhoushan 316022, China;
[3] Key Laboratory of Marine Materials and Related Technologies, Ningbo Institute of Materials Technology and Engineering, Chinese Academy of Sciences;
[4] Shandong Special Equipment Inspection Institute Lute Inspection&Testing Co. Ltd, Jinan 250100, China
[*]E-mail: danielxdzhao@aliyun.com; kittyangj@163.com

Received: 16 October 2018 / *Accepted:* 14 November 2018 / *Published:* 30 November 2018

In this paper, the corrosion behavior of 16Mn steel in sterile medium and three hydrocarbon degrading bacteria containing environment was investigated by electrochemical impedance spectroscopy (EIS) and polarization curves. The results showed that self-corrosion current density of 16Mn steel in bacteria-containing medium was significantly much less than that in sterile medium, suggesting the corrosion was inhibited by the attachment of the bacteria to the surface of the steel substrate. In the three bacteria-containing media, the difference of corrosion current densities resulted from the surface hydrophobicity of bacterial cells or ability to degrade organic matter.

Keywords: Microbiologically influenced corrosion (MIC), hydrocarbon degrading bacteria, Electrochemical impedance spectroscopy(EIS).

1. INTRODUCTION

Microbiologically influenced corrosion (MIC) is one of the most significant ways among the many influence factors resulting in the damage of steel oil storage tanks [1]. It is a kind of electrochemical corrosion mainly caused by microorganism or microbial metabolic activity. The adhesion of biofilms attached to the surface of the material is responsible for the MIC [2~3]. In recent years, it is found that the strength of the steel tanks is impacted by the fatigue damage caused by MIC,

which greatly affects the service life of the tanks. Oil leakage caused by corrosion perforation of the oil storage tanks can easily lead to series of dangerous accidents [4~5]. Sulfate reducing bacteria(SRB) are the most harmful and widely studied among all bacteria related to MIC. As far as oil storage tank is concerned, SRB cause damage to tank equipment as well as pollute the oil and lower its quality. A number of studies have been carried out to discuss about the corrosion mechanism under the influence of microorganisms represented by SRB [6~11]. For example, Cord-Ruwisch [12] showed corrosion process of microorganisms on steel surface of oil storage tanks by studying the growth characteristics of SRB and controlling its behavior in oil products. MIC caused by other bacteria also attracts attention of scholars. Rajasekar A [13] studied the corrosion effect of diesel biodegrading bacteria, *Serratia marcescens* (ACE2) and *Bacillus cereus* (ACE4), on carbon steel by EIS analysis and weight loss method. Petroleum hydrocarbon degrading bacteria are microorganisms that use petroleum components and degradation products as their main carbon and energy source, widely existing in the oil spill environment. The surfactant produced by hydrocarbon degrading bacteria first emulsifies and then disperses grease to form tiny oil droplets suspended in water, or the surfactant lowers the surface tension between oil droplets and cell walls of hydrocarbon degrading bacteria to make tiny oil droplets adsorbed on the surface of bacteria. Finally they enter the petroleum hydrocarbon degrading bacteria bodies and then decompose or accumulate.

Since usually there is a mixture of sedimentary water and oil in the bottom of oil tank, the presence of a variety of hydrocarbon degrading bacteria is common and inevitably has a certain influence on MIC. However, less research has been carried out in this field up to now. In this paper, three kinds of hydrocarbon degrading bacteria were isolated from the natural environment, and the corrosion behavior of 16Mn steel in the bacteria-containing media was investigated by electrochemical impedance spectroscopy (EIS) and polarization curves.

2. EXPERIMENTAL SECTION

2.1 Materials

For the electrochemical measurements, the working electrodes used in this work were cut from a 16Mn steel plate, and the composition is as follows(wt.%): 0.19 C, 0.35 Si, 1.50Mn, 0.05 Cr, 0.016 P, 0.019 S, 0.1 Ni, 0.05 Cu, Fe balance. The metal coupons were sealed with epoxy resin, leaving a geometrical surface area of 1 cm^2 exposed to the electrolyte. Before the experiment, the working surfaces were abraded with a series of silicon carbide papers (up to 1200), and then washed with distilled water and degreased in acetone and dried. The electrode was kept in a deoxygenated chamber, sterilising by ultraviolet lamp for 30 min prior to testing.

2.2 The bacteria and culture

Hydrocarbon degrading bacteria used in this study were isolated from sedimentary water in the bottom of oil tank in order to investigate MIC of the 16Mn steel in the microbial environment. A broth agar medium was used for the enrichment culture, which contained 3.0g beef extract, 10g peptone, 25g NaCl, 10~15g agar in 1000ml deionized water. The crude oil medium contained 4.0g crude oil, 0.2g

KH_2PO_4, 0.2g NH_4NO_3 in 1 L aged seawater. Both the media (high temperature resistant) was sterilized using high pressure steam sterilizer (121℃, 30 min).

The colonies of bacteria were cultured in broth agar media, selected for plate streaking cultivation and then placed in an incubator at 25℃ for 1~2 days. The above steps were repeated until single pure strain was obtained. The selected hydrocarbon degrading bacteria were inoculated in crude oil media at a rate of 2 mL/100 mL, and cultured for 7 days at 150 r/min in a constant temperature shaking incubatorat at 25℃. By sequencing, the bacteria were identified as *Exiguobacterium sp.*(ASW-1, in short below), *Alcaligenes sp.* (ASW-2) and *Bacillus sp.*(ASW-3), respectively.

2.3 Electrochemical measurement

The electrochemical impedance spectroscopy(EIS) was used to investigate the electrochemical properties of the 16Mn steel after 1d, 3d, 5d, 7d immersion in the microbial-extract solution with hydrocarbon degrading bacteria. The polarization curves were tested after 7 days. All experiments were performed in a classical three-electrode cell, with a platinum electrode used as the counter electrode, and a saturated calomel electrode (SCE) as the reference electrode. All tests were operated using an EG&G Parstat 2273 electrochemical system. Electrochemical impedance spectroscopy was performed in the frequency range from 0.001 Hz to 100 kHz and the amplitude of the sinusoidal voltage signal was 10 mV. The EIS data obtained were modeled and simulated using the Zsimpwin software supplied by the Parstat 2273. The polarization curve was tested in a scanning range of -350mV to +350mV at a scanning rate of 0.333 mV/s.

3. RESULTS AND DISCUSSION

3.1 EIS analysis of 16Mn steel in sterile medium

Fig.1 shows the Nyquist and Bode diagrams of the 16Mn steel in sterile medium after different immersion time.

During immersion, high frequency region showed the characteristic impedance semicircle controlled by charge transfer and low frequency region showed the characteristic straight line controlled by diffusion on the basis of Nyquist diagram. It was reported that the impedance modulus at the lowest frequency in Bode diagram could be used as a semi-quantitative indicator of corrosion behavior [14]. In the initial stage of immersion, the capacitive loop was the smallest. Then the radius of the capacitive loop increased with time, indicating that the gradual formation of biofilm or corrosion product had a protective effect on the metal substrate. The change of diffusion impedance in middle and low frequency regions showed the process was changed gradually from a charge transfer-controlled transition to a diffusion-controlled one.

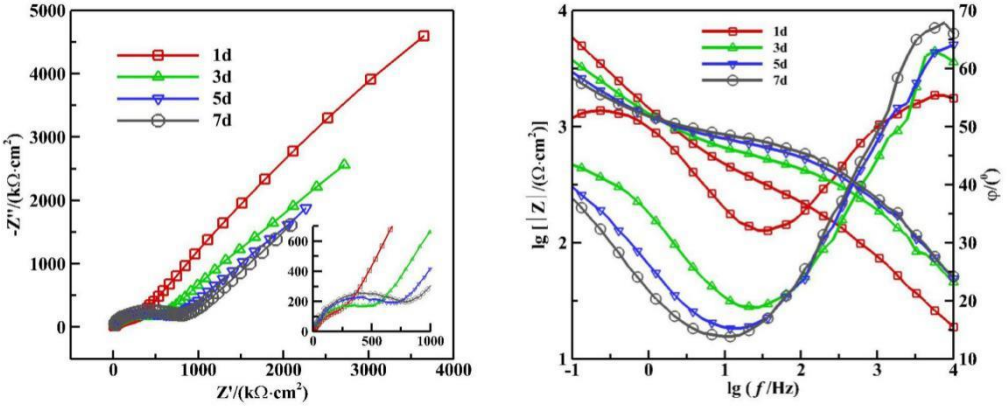

Figure 1. The Nyquist and Bode diagrams of 16Mn steel in sterile medium over immersion time

To further analyze the corrosion mechanism of the steel in sterile medium, EIS results were fitted with equivalent circuit, as shown in Fig.2 and the fitting result was summarized in Tab.1. In the equivalent circuit model, R_s represents an electrolyte resistance, R_c and Q_c represent a resistance and a capacitance of the corrosion product film, R_{ct} and Q_{dl} represent a charge transfer resistance and a double layer capacitance, respectively, R_w represents a diffusion resistance, and n represents coefficient of dispersion. Hereinto, CPE is considered to represent a circuit parameter with limiting behavior as a capacitor for n=1, a resistor for n=0, and an inductor for n = -1 [15]. The equivalent circuit shown in Fig.2 was used to fit the results for the samples after 7d of immersion. In the initial stage, the corrosive media had not penetrated the substrate because of the film formed on the steel surface. The corrosive media reached to the metallic substrate over time, shown as the variation of R_{ct} value. The result was consistent with the change of the capacitive loop.

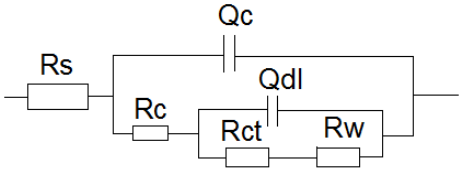

Figure 2. The equivalent circuit model used to fit the EIS experimental data for 16Mn steel immersed in sterile medium

Table 1. Fitting parameters derived from equivalent circuit in sterile medium

Immersion time	R_s ($\Omega \cdot cm^2$)	$Q_c \times 10^{-4}$ ($\Omega^{-1} \cdot cm^{-2}$)	n_1	R_c ($\Omega \cdot cm^2$)	$Q_{dl} \times 10^{-4}$ ($\Omega^{-1} \cdot cm^{-2}$)	n_2	R_{ct} ($\Omega \cdot cm^2$)	$W \times 10^{-4}$ ($\Omega \cdot cm^2$)
1d	0.67	0.48	0.66	299.1	2.39	0.66	3.82E4	152.9
3d	1×10^{-7}	0.09	0.72	388.3	1.83	0.66	124.7	3.03
5d	1×10^{-7}	0.08	0.72	530.7	6.58	0.54	223.1	3.13
7d	0.44	0.03	0.81	405	0.04	0.97	166.9	7.79

3.2 EIS analysis of 16Mn steel in ASW-1 medium

Fig.3 shows the Nyquist and Bode diagrams of the 16Mn steel in ASW-1 medium. As a function of time, the capacitive loop radius increased first and then decreased in the Nyquist diagram during the immersion period, while it showed two time constants in the Bode diagram. The EIS showed the characteristic of the single capacitive loop and diffusion control after ASW-1 inoculation for 1d. At the moment, the amount of bacteria was low since they were in a period of growth retardation, so the surface of steel electrode was mainly covered by the adsorption film of culture medium and biofilm [16]. With proliferation of the bacteria, the corrosion product layer began to form on the surface of 16Mn steel, and the film was complete so as to protect the substrate from being easily corroded. On the fifth day, the maximum value of the capacitive loop appeared, indicating the lowest corrosion tendency. As shown from the Bode diagram in Fig.3, the maximum phase angle shifted to the low-frequency direction with the time of cultivation, revealing that the biofilm layer was unstable and easily broken [17]. Then the biofilm on the surface of the samples falls off and the surface was uneven covered when the ASW-1 gradually entered the growth decline period. Then the capacitive loop radius became smaller while corrosion tendency increased although it was not obviously shown in the EIS curves.

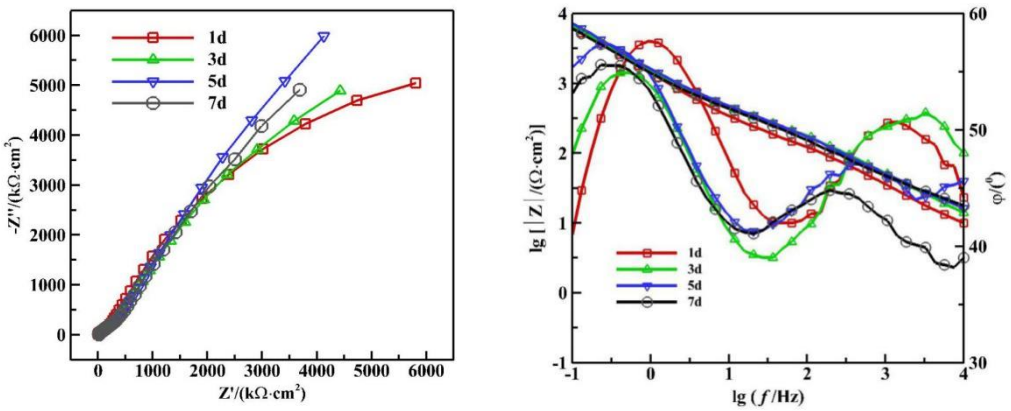

Figure 3. The Nyquist and Bode diagrams of 16Mn steel in ASW-1 medium over immersion time

EIS results were fitted with equivalent circuit, as shown in Fig.4 and the fitting result was summarized in Tab.2. Equivalent circuit parameters represented the same as mentioned above.

From the fitting results we can see that the Q_c value was gradually increasing due to corrosive media penetrating the inhomogenous layer on 16Mn steel surface. At the same time, the R_{ct} and Q_{dl} value also showed an increasing trend, indicating the corrosion products inhibited the corrosion of 16Mn steel to a certain extent. Then the R_{ct} value decreased, showing the corrosive media penetrated the corrosion product layer and accelerated the corrosion. In addition, the value of dispersion coefficient, n, was less than 1, representing a non-ideal capacitance, which resulted from the inhomogeneous surface film and the increase of transverse and vertical heterogeneity [18~21].

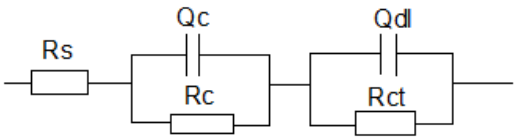

Figure 4. The equivalent circuit model used to fit the EIS experimental data for 16Mn steel immersed in ASW-1 medium

Table 2. Fitting parameters derived from equivalent circuit in ASW-1 medium

Immersion time	R_s ($\Omega \cdot cm^2$)	$Q_c \times 10^{-4}$ ($\Omega^{-1} \cdot cm^{-2}$)	n_1	R_c ($k\Omega \cdot cm^2$)	$Q_{dl} \times 10^{-4}$ ($\Omega^{-1} \cdot cm^{-2}$)	n_2	R_{ct} ($k\Omega \cdot cm^2$)
1d	2.67	1.76	0.76	12.49	1.18	0.64	0.16
3d	1.15	2.33	0.74	16.69	1.35	0.61	0.24
5d	1.88	2.30	0.76	28.32	2.33	0.55	0.36
7d	3.86	2.72	0.77	19.44	3.10	0.52	0.35

3.3 EIS analysis of 16Mn steel in ASW-2 medium

Fig.5 shows the Nyquist and Bode diagrams of the 16Mn steel in ASW-2 medium. Similar to the above results, the high frequency region showed the single capacitive loop and middle-low frequency region showed the diffusion impedance during immersion. After 1d, biofilm on the surface of 16Mn steel was incomplete with little amount of bacteria. It showed a small capacitive impedance loop radius in Nyquist curves. The capacitive arc radius increased with time although not obviously. The EIS results were fitted with equivalent circuit, as shown in Fig.6 and the fitting parameters were summarized in Tab.3.

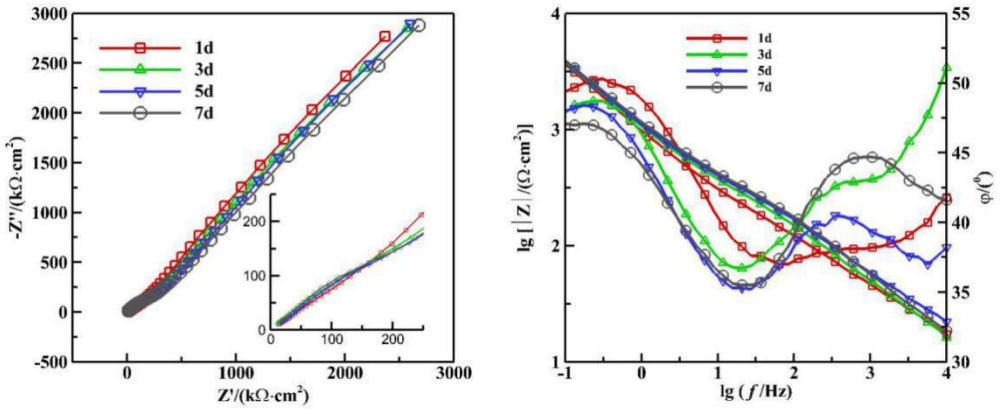

Figure 5. The Nyquist and Bode diagrams of 16Mn steel in ASW-2 medium over immersion time

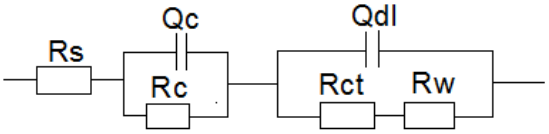

Figure 6. The equivalent circuit model used to fit the EIS experimental data for 16Mn steel immersed in ASW-2 medium

Table 3. Fitting parameters derived from equivalent circuit in ASW-2 medium

Immersion time	R_s ($\Omega \cdot cm^2$)	$Q_C \times 10^{-4}$ ($\Omega^{-1} \cdot cm^{-2}$)	n_1	R_C ($\Omega \cdot cm^2$)	$Q_{dl} \times 10^{-4}$ ($\Omega^{-1} \cdot cm^{-2}$)	n_2	R_{ct} ($\Omega \cdot cm^2$)	$W \times 10^{-4}$ ($\Omega \cdot cm^2$)
1d	1×10^{-7}	4.91	0.45	312.2	1.57	0.94	89.93	3.78
3d	9×10^{-6}	3.11	0.51	245.9	4.19	0.66	1380	4.99
5d	3.73	2.67	0.50	512.4	2.18	0.96	555.3	3.65
7d	2.74	1.61	0.56	340.2	1.70	0.90	474.4	3.58

3.4 EIS analysis of 16Mn steel in ASW-3 medium

Fig.7 shows the Nyquist and Bode diagrams of the 16Mn steel in ASW-3 medium. There were two capacitive arcs in the Nyquist diagram and two time constants in the Bode diagram during the immersion. Thereinto, the capacitive arc in the high-frequency region corresponded to the film resistance and capacitance of corrosion products, while the capacitive arcs in the middle and low frequency area corresponded to the charge transfer resistance and double layer electric capacitance between the metal substrate and the film. The value of capacitive loop radius and module value in the low frequency area gradually decreased with the immersion time in ASW-3 medium, indicating the corrosion trend of 16Mn steel increased. Particularly, it was obvious that capacitive loop radius decreased after 7d in ASW-3 medium.

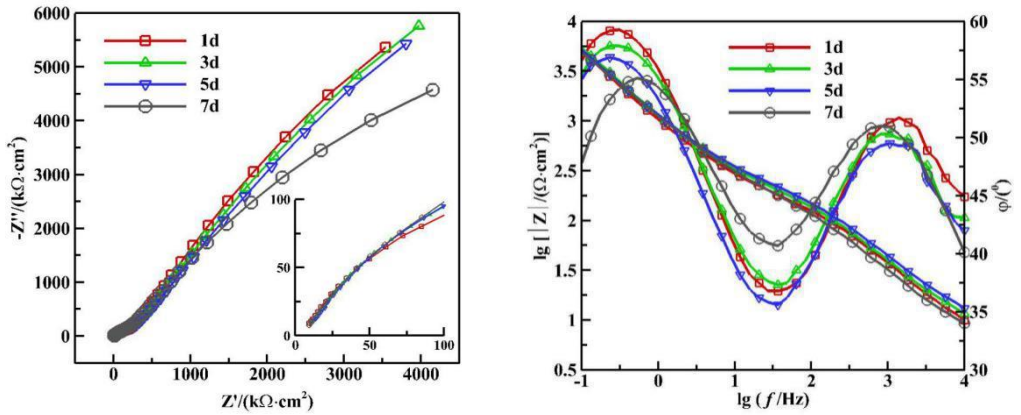

Figure 7. The Nyquist and Bode diagrams of 16Mn steel in ASW-3 medium over immersion time

The EIS results are fitted with equivalent circuit, as shown in Fig.8 and the fitting parameters are summarized in Tab.4. As shown in Tab.4, the total resistance after immersion of 1d, 3d, 5d changed little, corresponding to the small difference among the three radius of capacitive loops in Nyquist diagram. However, the total resistance reduced to its minimum value, revealing the acceleration of the corrosion rate after 7d and meanwhile, the capacitance arc radius and low-frequency module value were significantly smaller.

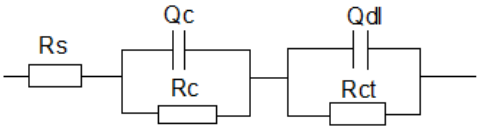

Figure 8. The equivalent circuit model used to fit the EIS experimental data for 16Mn steel immersed in ASW-3 medium

Table 4. Fitting parameters derived from equivalent circuit in ASW-3 medium

Immersion time	R_s ($\Omega \cdot cm^2$)	$Q_c \times 10^{-4}$ ($\Omega^{-1} \cdot cm^{-2}$)	n_1	R_c ($k\Omega \cdot cm^2$)	$Q_{dl} \times 10^{-4}$ ($\Omega^{-1} \cdot cm^{-2}$)	n_2	R_{ct} ($k\Omega \cdot cm^2$)
1d	3.22	2.74	0.72	43.8	0.83	0.68	0.17
3d	4.24	2.47	0.72	41.59	0.88	0.67	0.19
5d	4.75	0.81	0.66	0.21	0.26	0.71	43.89
7d	3.76	2.52	0.71	17.03	1.19	0.67	0.16

3.5 Polarization curves analysis

The potentiodynamic polarization curves of 16Mn steel immersed in ASW-1, ASW-2, ASW-3 and sterile medium after 7 days were shown in Fig.9, respectively. And the corresponding corrosion potential (E_{corr}) and corrosion current density (i_{corr}) calculated from Tafel plots were summarized in Tab.5. In general, a higher E_{corr} and lower i_{corr} indicated a better corrosion protection. It could be seen that 16Mn steel immersed in sterile medium possessed the highest corrosion potential (E_{corr} =−0.752V) and the lowest corrosion current density (i_{corr} =2.454μA·cm^{-2}). The values of corrosion potential and corrosion current density were smaller than the 16Mn steel immersed in three kinds of bacteria media, which indicated the hydrocarbon degrading bacteria could inhibit the corrosion of 16Mn steel to a certain extent. The corrosive ions of the electrolyte solution in the sterile medium directly contacted with the metal material, causing the corrosion behavior of the metal surface. By comparing the slope of the anodic polarization curve (185 mV·dec^{-1}) and that of the cathodic polarization curve (120 mV·dec^{-1}), the anodic slope was larger, showing the corrosion reaction was controlled by anode reaction. When the steels were immersed in the media containing the hydrocarbon degrading bacteria, the bacteria were likely to adhere to the surface of the material and inhibit the direct contact of the corrosive ions with the metal substrate. To further analyze and compare the corrosion performance of 16Mn steel immersed in the media with three kinds of hydrocarbon degrading bacteria (ASW-1, ASW-2, ASW-3), we also could make some conclusions by the related fitting data. From the Tab.5, we could see the different hydrocarbon degrading

bacteria had different effects on 16Mn steel. The 16Mn steel had a large corrosion effect in media containing ASW-3. It had the largest corrosion potential (E_{corr} =−0.737V) and self-corrosion current density (i_{corr} =1.028μA·cm^{-2}) among the three bacteria. Simultaneously, according to the slope of the anode (73 mV·dec^{-1}) and cathode (60 mV·dec^{-1}), the corrosion reaction could be judged as mixed control. The 16Mn steel immersed in media with ASW-1 and ASW-2 had similar corrosion behavior. It might be that the two isolated bacteria from crude had similar activities. In addition, the integrity of the bacterial biofilm could inhibit the corrosion of 16Mn steel better. Thus, the integrity of ASW-3 biofilm attached to the surface of metallic materials determined the corrosion rate of 16Mn steel. When the biofilm attached to the surface was destroyed, the water, dissolved oxygen, corrosive ions would pass through the crack causing corrosive reaction.

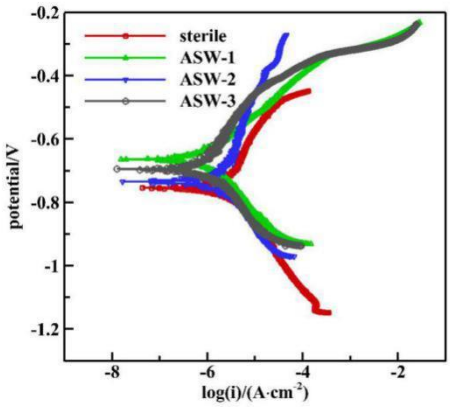

Figure 9. The polarization curves of 16Mn steel immersed in different media after 7d

Table 5. Corrosion parameters of 16Mn steel immersed in different media after 7d

Medium	E_{corr} (V,vs.SCE)	i_{corr} (μA·cm^{-2})	β_a (mV·dec^{-1})	-β_c (mV·dec^{-1})
Sterile	-0.752	2.454	185	120
ASW-1	-0.671	0.489	76	28
ASW-2	-0.699	0.419	6	26
ASW-3	-0.737	1.028	73	60

3.6 Discussion

Hydrocarbons are common in the petroleum, and the degradation of hydrocarbons by microorganisms becomes a primary means for repairing pollution of petroleum hydrocarbon [22]. The hydrophobicity of cell surface of petroleum hydrocarbon degrading bacteria is an important property of such microorganisms, which directly affects the functional efficiency in many biological processes especially the absorption between microorganisms and other substances [23] as well as impacts on the

material corrosion. As mentioned above, surface active substances produced by hydrocarbon degrading bacteria can reduce the surface tension between the oil droplets and bacterial cell wall. In this way, the fine oil droplet is adsorbed on the bacterial surface. When the bacteria are adsorbed on the surface of the steel substrate, the effective contact of corrosive media with the substrate is also reduced.

Compared the corrosion behavior of 16Mn steel under the influence of three kinds of hydrocarbon degrading bacteria with the sterile environment, the corrosion process was inhibited to a certain extent for the adsorption of hydrocarbon degrading bacteria on the surface of 16Mn steel. The variation of corrosion current density showed the different effects of different bacteria on the corrosion of 16Mn steel. From the literature, although the metabolic activity and its metabolite of hydrocarbon degrading bacteria were not directly involved in the corrosion process, the surface hydrophobicity of bacteria had high correlation with its degradability [24-25]. At the same time, the hydrophobicity was related to the microbial corrosion of materials.

4. CONCLUSION

The electrochemical corrosion behavior of 16Mn steel in the presence of three different hydrocarbon degrading bacteria were studied compared with that in sterile medium. During the experiment period, the corrosion rate of 16Mn steel was obviously higher in sterile media than that in the other three bacteria-containing media, showing that the bacteria had an inhibitory effect on the corrosion of 16Mn steel compared to the sterile medium. In the three kinds of bacteria-containing media, the 16Mn steel had the largest corrosion current density in ASW-2 medium. The difference of corrosion current density resulted from the surface hydrophobicity, as well as the degradability of bacteria.

ACKNOWLEDGMENTS
This research was supported by Foundation of Key Laboratory of Marine Materials and Related Technologies, Ningbo Institute of Materials Technology and Engineering, Chinese Academy of Sciences (Grant No.2017Z01). The support from Scientific Research Foundation of Yantai University (Grant No.HX17B38) is also gratefully acknowledged.

Reference

1. B.J. Little, P.A. Wagner and F. Mansfeld, *Electrochim. Acta.*, 37(1992)2185.
2. B.J. Little, P.A. Wagner and F. Mansfeld, *Microbiologically Influenced Corrosion*, (2008) Springer London, U. K.
3. R. Javaherdashti, *Anti-Corros. Method. M.*, 46(1999)173.
4. J. Dong, Q. Li, *Guangdong Chem. Ind.*, 40(2013)129.
5. L. Wang, Z. Wang and C. Yang, *Corros. Prot. Pe. Ind.*, 3(2016)13.
6. I.B. Beech and S. A. Campbell, *Electrochim. Acta.*, 54(2008)14.
7. E. Malard, D. Kervadec and O. Gil, *Electrochim. Acta.*, 54(2008)8.
8. R. Jeffrey and R. E. Melchers, *Corros. Sci.*, 45(2003)693.
9. N. Boudaud, M. Coton and E. Coton, *J. Appl. Microbiol.*, 109(2010)166.
10. R.E. Melchers, *Corros. Eng. Sci. Techn.*, 45(2010)257.

11. E. Ilhan-Sungur and A. Çotuk, *Corros. Sci.*, 52(2010)161.
12. R. Cord-Ruwisch, W. Kleinitz and F. Widdel, *J. Petrol. Technol.*, 39(1987)97.
13. A. Rajasekar, *Biodegradation and Bioconversion of Hydrocarbons*, (2017)Springer Singapore, Singapore.
14. M. Conradi, A. Kocijan and D. Kek-Merl, *Appl. Surf. Sci.*, 292(2014)432.
15. J.B. Jorcin, M.E. Orazem and N. Pébère, *Electrochim. Acta.*, 51(2006)1473.
16. H. Liu and T. Liu, *J. Chinese Soc. Corros. Prot.*, 60(2009)218.
17. D. Çetin, S. Bilgiç and S. Dönmez, *Mater. Corros.*, 58(2007)841.
18. G. Huang, K. Chan and H. Fang, *J. Electrochem. Soc.*, 151(2004)434.
19. K.M. Ismail, A. Jayaraman and T.K. Wood, *Electrochim. Acta.*, 44(1999)4685.
20. C. Xu, Y. Zhang and G. Cheng, *Mater. Charact.*, 59(2008)245.
21. A. Ghosh, B. Leonard and F. Sadeghi, *Wear.*, 307(2013)87.
22. S. Chakraborty, S. Mukherji and S. Mukherji, *Colloid. Surface. B.*, 78(2010)101.
23. V. Pruthi and S.S. Cameotra, *Biotechnology. Techniques.*, 11(1997)671.
24. M. Rosenberg, *Appl. Environ. Microb.*, 42(1981)375.
25. Y. Wang, J. Geng and G. Guo, *Chem. Eng. J.*, 172(2011)999.